THE JOURNAL OF PHYSICAL CHEMISTRY A

Article

Cite This: J. Phys. Chem. A 2018, 122, 2626−2633

pubs.acs.org/JPCA

Quasi-Classical Trajectory Dynamics Study of the $Cl(^2P) + C_2H_6 \rightarrow HCl(v,j) + C_2H_5$ Reaction. Comparison with Experiment

Joaquin Espinosa-Garcia,*[,†] Emilio Martinez-Nuñez,[‡] and Cipriano Rangel[†]

[†]Departamento de Química Física and Instituto de Computacion Cientifica Avanzada, Universidad de Extremadura, 06071 Badajoz, Spain

[‡]Departamento de Química Física, Universidad de Santiago de Compostela, Santiago de Compostela, Spain

ABSTRACT: To understand and simulate the dynamics behavior of the title reaction, QCT calculations were performed on a recently developed global analytical potential energy surface, PES-2017. These calculations combine the classical description of the dynamics with pseudoquantization in the reactants and products to perform a theoretical/experimental comparison on the same footing. Thus, in the products a series of constraints are included to analyze the HCl(v = 0,j) product, which is experimentally detected. At collision energies of 5.5 and 6.7 kcal mol^{-1} the largest fraction of available energy is deposited as translation, 67%, while the ethyl radical shows significant internal energy, 27%, and so it does not act as a spectator of the reaction, thus reproducing recent experimental evidence. The HCl(v=0,*j*) rotational distribution is cold, peaking at *j* = 2, only one unit hotter than experiment, which represents an error of 0.12 kcal mol^{-1}. At a collision energy of 5.5 kcal mol^{-1} product translational distribution is slightly hotter than experiment, but at 6.7 kcal mol^{-1} agreement with recent experiments is practically quantitative, suggesting that the first experiments should be revised. In addition, we observe that the HCl(v=0,*j*) scattering distribution shifts from isotropic at low values of *j* to backward at high values of *j*, which is in agreement with experimental data. Finally, no evidence was found for the "chattering" mechanism suggested to explain the low translational energy of the HCl product in the backward scattering region. In sum, agreement with experiments of a series of sensible dynamic properties permits us to be optimistic on the quality and accuracy of the theoretical tools used in the present work, QCT and PES-2017.

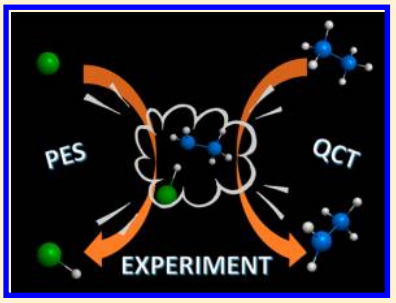

1. INTRODUCTION

Theoretical dynamics understanding of chemical reactivity requires two tools, the potential energy surface (PES) describing the nuclei motion in the field of the electrons, and the dynamics method (quantum mechanical, QM, or quasi-classical trajectory, QCT) describing the motion equations. Comparison with experiments represents a severe test of the quality of these tools, and in some cases shows experimental uncertainties and/or solves experimental controversies. Obviously, the theory/experiment comparison should be made on the same footing, i.e., with the same measured physical property in both cases. This fact is sometimes forgotten when QCT results (taking into account all the vibrational and rotational product states) are compared with fine state-to-state experiments.

In the present work, to complete the previous kinetic studies,[1] an exhaustive dynamics study was performed on the gas-phase hydrogen abstraction reaction

$$Cl(^2P) + C_2H_6 \rightarrow HCl(v,j) + C_2H_5$$

This is an example of a polyatomic system of medium size (nine bodies), difficult to study theoretically by using high-level ab initio calculations due to the expensive computational cost, which surpasses the paradigmatic, closely related, and well-studied $Cl(^2P) + CH_4$ reaction, permitting analysis of the dynamics role of the ethyl radical.

The title reaction is interesting for several reasons, related with the main aims of the present work: (i) Compared with the great volume of dynamics studies on smaller systems of the type X + CH_4 (X: H, O, halogens), there is less dynamics information. (ii) The title reaction presents a "central" transition state, where the application of Polanyi's rules[2] is less straightforward than in reactions with "early" or "late" transition states. (iii) Experimental controversies exist on the internal energy deposited in the ethyl radical, which condition the scattering distributions and therefore the dynamics behavior.[3−10] By using single beam experiments at a collision energy of 5.5 kcal mol^{-1}, Kandel et al.[3,4] in 1996−1998, and later Bass et al.[6] in 2003 studied this reaction by employing the photoloc method. However, both groups used different analysis techniques, obtaining different results on the available energy deposited into the ethyl radical. Whereas Kandel et al. reported only 7%, concluding that the ethyl radical acts as a spectator, Bass et al. obtained a value of 22%, concluding that it plays an important role in the dynamics. Later, in 2006, Suits and co-workers[8,9] used crossed molecular beams at a collision energy of 6.7 kcal mol^{-1}, concluding that the ethyl radical presents significant internal energy, ∼30% of the available energy, in

Received: January 8, 2018
Revised: February 28, 2018
Published: February 28, 2018

DOI: 10.1021/acs.jpca.8b00149
J. Phys. Chem. A 2018, 122, 2626−2633

close agreement with Bass et al. (iv) Finally, comparatively fewer theoretical dynamics studies have been performed on the title reaction,[11−14] due probably to the high computational cost. In general, QCT calculations were performed on different PESs of low level, semiempirically or on-the-fly at the Hartree−Fock ab initio level, with a very low number of trajectories run, 2000−20 000, which leads to important statistical errors. The most recent and complete study was performed by Greaves et al.[14] in 2008, who reproduced the product translational and angular experimental distributions but found that the HCl(j) rotational excitation is 2−3 units hotter than experiment with a large tail at high HCl(j) values, which corresponds to experimentally unassailable energies.

In this work we present dynamics results of the title reaction using QCT calculations based on the recently developed full-dimensional analytical PES, PES-2017,[1] which is based on high-level ab initio calculations. The present study improves the description of the reactive system with respect to previous theoretical studies, first, because the new PES-2017 is based exclusively on high-level ab initio calculations at the CCSD(T) =FC/aug-cc-pVTZ (and higher basis sets) and, second, because some constraints are included in the final analysis of the reactive trajectories to simulate the experimental conditions. It is organized as follows: the theoretical tools used, potential energy surface and QCT calculations, are presented in section 2. Section 3 contains the results and the comparison with experiments and previous theoretical studies. Finally, section 4 summarizes the main conclusions.

2. THEORETICAL TOOLS

Theoretical dynamic studies require knowledge of the potential energy surface, description of the nuclei motion in the field of the electrons, and a dynamics method, which in this case consists of quasi-classical trajectory calculations, given the dimensionality of the reactive system. These will now be analyzed independently.

2A. Potential Energy Surface. The Cl(^{2}P) + C_2H_6 → HCl(v,j) + C_2H_5 gas-phase hydrogen abstraction reaction is a nine-body system with 21 degrees of freedom, which represents a real theoretical challenge. On the basis of high-level ab initio calculations at the CCSD(T)=FC/aug-cc-pVTZ level and higher, we recently developed an original analytical PES for this system, named PES-2017.[1] Intuitive chemical concepts such as stretching, bending, and torsional motions were represented by using valence bond (VB) functions augmented with molecular mechanics (MM) functions. This VB/MM functional form depends on 60 adjustable parameters to fit the ab initio input data. This was explained in detail in our previous paper[1] and so will not be repeated here.

For the sake of clarity, Figure 1 shows the energetic diagram with the stationary points along the reaction path. The exothermicity of the reaction, $\Delta H_R(0K)$ = −3.55 kcal mol^{-1}, reproduces the experimental information (298 K),[15,16] −2.67 ± 0.5 and −2.08 ± 0.39 kcal mol^{-1}, whereas the barrier height, 2.44 kcal mol^{-1} and the stability of the intermediate complexes, −0.64 and −1.97 kcal mol^{-1} for the reactant and product complexes (the latter with respect to the products), respectively, reproduce the ab initio information used in the fitting process and previous theoretical calculations.[11,14] A very important issue in this system is the effect of spin−orbit coupling due to the presence of the Cl(^{2}P) reactant. This issue was analyzed in depth in our previous paper to explain the kinetics behavior,[1] especially at low temperatures, where the theory/experiment discrepancies are greater. However, given the heavy-light-heavy mass combination, a priori tunnelling should play a significant role at low temperatures. However, given that this reaction presents a negative adiabatic barrier (Figure 1), in our previous paper[1] we showed that this effect is negligible. In addition to the previous tests, the torsional motion about the C−C bond and the bending motion about the C···H′···Cl bonds in the saddle point also reproduce the ab initio input data. Therefore, these stringent tests lend confidence to the new PES-2017 and permit us to be optimiztic about its use in dynamics calculations.

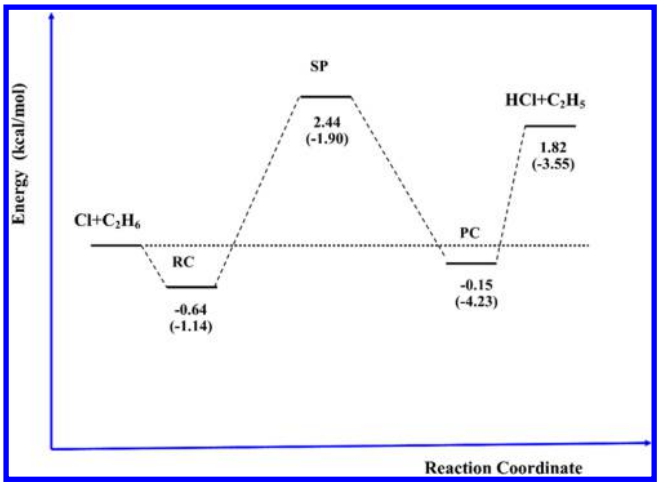

Figure 1. Energy schematic diagram of the stationary point for the Cl + C_2H_6 reaction using PES-2017. RC, SP, and PC represent, respectively, the reactant complex, the saddle point, and the product complex. The zero-point energy corrected values appear in parentheses. Dotted line: reactants level zero.

2B. Trajectory Calculations. QCT calculations as implemented in the VENUS-96 code[17,18] were performed on the new PES-2017 surface, with appropriate initial conditions to reproduce the experiments at different collision energies. The trajectories were initiated and stopped at C−Cl distances of 10 and 15 Å, respectively, i.e., asymptotic reactant and product regions where molecular interactions are negligible. Using a step of 0.1 fs, the scattering parameters, such as impact parameter, vibrational phases, and spatial orientation of the reactants, were selected from a Monte Carlo approach. To simulate the molecular beam experiments, the ethane reactant rotational energy was chosen by thermal sampling at cold 10 K, where only the ZPE in the vibrational energy was included, 45.45 kcal mol^{-1}. Collision energies in the range 1.0−10.0 kcalmol^{-1} were analyzed, with special attention to the values at 5.5 and 6.7 kcal mol^{-1}, which present more experimental information.[3,4,8,9] The analytical functional form of the PES-2017 permitted us to run a large number of trajectories. A total of 10^6 trajectories were run at each collision energy, which contrasts with the reduced number of trajectories, $<2 \times 10^4$, used in previous theoretical studies. This large number of trajectories gives small or negligible statistical errors (<3%), which for reasons of clarity are not shown in the Results. At each collision energy, the maximum impact parameter, b_{max}, was obtained with batches of 5000 trajectories. The values vary from 5.7 Å at 1.0 kcal mol^{-1} to 3.7 Å at 10.0 kcal mol^{-1}. In total, more than 7×10^6 trajectories were analyzed.

We begin the analysis of the reactive trajectories by considering the reaction cross section, σ_r (Å^2), given by

DOI: 10.1021/acs.jpca.8b00149
J. Phys. Chem. A 2018, 122, 2626−2633

$$\sigma_r = \pi b_{max}^2 \frac{N_r}{N_T} \quad (1)$$

where N_r and N_T represent, respectively, the number of reactive and total trajectories at each collision energy. However, an important limitation of the QCT calculations is the ZPE violation problem, i.e., when the products appear with vibrational energy below their ZPE. To solve this problem, we discarded all reactive trajectories where both products, HCl and C_2H_5, presented a vibrational energy below their ZPE, 4.2 and 35.8 kcal mol^{-1}, respectively (double zero-point energy approach, DZPE). This passive method leads to a drastic reduction in the number of reactive trajectories, but it includes a "quantum" spirit in the analysis of the results. For instance, at a collision energy of 5.5 kcal mol^{-1}, from 261 000 to 20 600, i.e., more than 90% of reactive trajectories, were discarded. The DZPE approach (together with other constraints in the QCT outcome) permitted simulation of fine velocity map imaging (VMI) experiments performed by Liu for the OH + CH_4 (and isotopic analogues)[19−21] and by Liu and Yang for the F + CHD_3(v=0,1)[22−24] reactions at a very high level of detail.[25−27] Therefore, on the basis of the previous experience, the DZPE approach seems a valid scheme in the analysis of polyatomic reactions.

In addition, the following product quantities of interest in the dynamics study were obtained from the QCT outcome: vibrational and rotational energies of the HCl and C_2H_5; vibrational and rotational actions of the diatomic product, HCl(a_v,a_j); the relative translational energy, E_{trans}, between the products; and the scattering angle, θ, between the HCl product and the incident Cl reactant. Given that QCT calculations are classical in nature, rotational and vibrational actions are continuous, and to "pseudo-quantize" them, they are rounded to the nearest integer value, HCl(v,j). The velocities of the products within the laboratory (LAB) frame are obtained from E_{trans} by

$$v_{HCl} = \left[\frac{2E_{trans}}{\mu}\right]^{1/2} \quad (2)$$

where μ is the reduced mass. Product angular distribution, PAD (determined from the final HCl and initial Cl velocity vectors), is measured by the differential cross section, DCS,

$$\frac{d\sigma_r}{d\Omega} = \frac{\sigma_r P(\theta)}{2\pi \sin\theta} \quad (3)$$

which represents the variation of the reaction cross section with respect to the solid angle (Ω), where $P(\theta)$ is obtained by counting the number of reactive trajectories at intervals of 5° in the range [0, π]. To compare with the continuously varying experimental measures, an efficient and elegant alternative is expansion in Legendre polynomials[28]

$$\frac{d\sigma_r}{d\Omega} = \left(\frac{\sigma_r}{2\pi}\right)\sum_n \frac{2n+1}{2} a_n P_n(\cos\theta) \quad (4)$$

where $P_n(\cos\theta)$ represents the normalized Legendre polynomial of order n, and

$$a_n = \langle P_n(\cos\theta)\rangle = \frac{1}{N_r}\sum_{i=1}^{N_r} P_n(\cos\theta^{(i)}) \quad (5)$$

denotes the Legendre moments, i.e., the average over the reactive trajectories, with $\cos\theta^{(i)}$ being the value in trajectory i.

Finally, to simulate the experimental conditions and, therefore, to perform a theory/experiment comparison on the same footing, it was necessary to include some constraints in the QCT analysis, in addition to the ZPE criterion in the products previously noted. Experimentally, the HCl(v=0) vibrational ground state was detected, and Rudic et al.[12] observed that the energy deposited in the ethyl radical was practically as rotation; i.e., the ethyl radical appears also in its vibrational ground state, C_2H_5(v=0). Therefore, the following energy constraints were taken into account:

(i) The ZPE of HCl is 4.2 kcal mol^{-1}, and it is permitted to vary in the unit range [ZPE−0.5, ZPE+0.5]. So, we take into account only the reactive trajectories in the range 4.2−4.7 kcal mol^{-1}. This is equivalent to considering that only values of HCl(a_v) in the range [v−0.15, v+0.15] contribute to the population of the HCl(v) vibrational level, which is a more stringent criterion than the unit range [v+0.5, v−0.5] used in the standard binning approach. We believe that this energetic constraint is acceptable for this reaction with nine bodies, because the more severe Gaussian binning method would drastically reduce the number of reactive trajectories.

(ii) Simultaneously, the ZPE of C_2H_5 is 35.8 kcal mol^{-1}, and the energy corresponding to one quantum in the lowest vibrational mode (229 cm^{-1}) is 0.65 kcal mol^{-1}. We consider therefore only reactive trajectories in the range 35.8−36.5 kcal mol^{-1}.

Obviously, these are very stringent constraints that bring the classical QCT results closer to a "quantum spirit" analysis and to the experimental conditions.

3. RESULTS AND DISCUSION

At 5.5 and 6.7 kcal mol^{-1} of collision energy, practically all reactive trajectories were found in the HCl vibrational ground state, HCl(v=0), 98 and 96%, respectively, in close agreement with the experimental evidence.[3,4] In the following subsections we analyze different dynamic properties, comparing the QCT results with experiment and/or previous theoretical results.

3A. Excitation Function. The QCT excitation function, which represents the reaction cross section as a function of the collision energy, is represented in Figure 2 in the energy range 1.0−10.0 kcal mol^{-1}. Unfortunately, neither experimental nor theoretical data are available for comparison. This function increases with collision energy, which is the typical behavior of reactions with barrier and reflects a relatively tight-bend transition-state structure, C···H′···Cl. With a small, but positive, activation energy,[1] +0.3 kcal mol^{-1}, this is the expected behavior, in accordance with the line-of-center model. Figure 2 also includes the excitation function considering all reactive trajectories, where σ_r is scaled by a factor 0.1 to use the same scale. Both functions show similar behaviors, indicating that this dynamics property is insensitive to the constraints in the QCT calculations. The only effect is the obvious decreases of the absolute values (by a factor of about 10). Note that, as expected, the effect of the constraints is more important at low collision energies.

3B. Product Energy Partitioning. For a direct comparison with available experimental data, QCT product energy partitioning at 5.5 and 6.7 kcal mol^{-1} is listed in Table 1 for the HCl(v=0,j) product. Given the heavy-light-heavy mass combination, the transfer from reactant to product translational energy is favored, which has a kinematic origin. The largest

DOI: 10.1021/acs.jpca.8b00149
J. Phys. Chem. A 2018, 122, 2626−2633

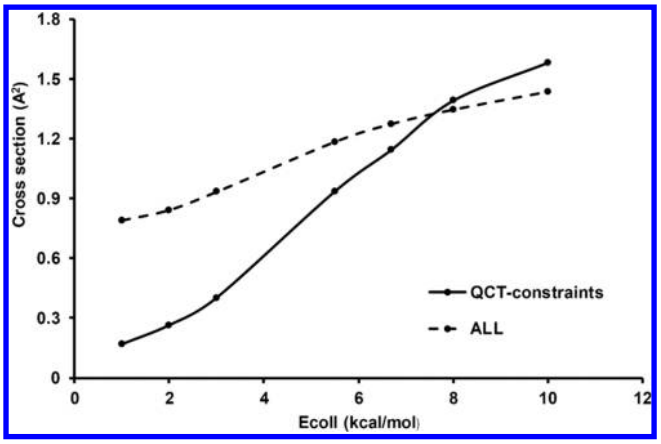

Figure 2. Reaction cross section (Å^2) as a function of the collision energy (kcal mol^{-1}). Seven values were calculated with statistical errors <3% and are not represented. Note that the continuous curves are a guide to eye: solid line, using reactive trajectories with QCT-constraints; dashed line, using all reactive trajectories scaled by a factor 0.1.

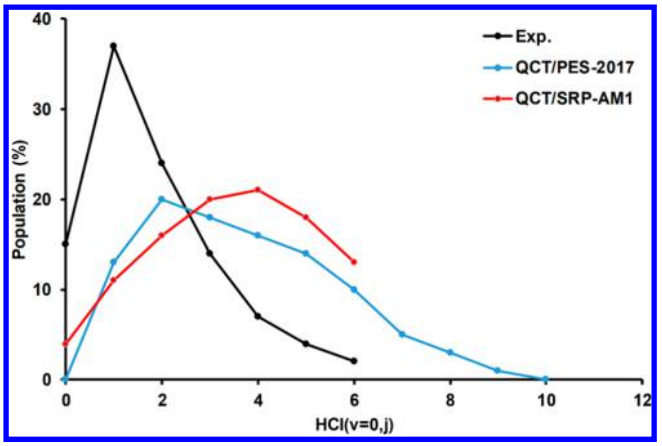

Figure 3. HCl(v=0,j) rotational distribution at E_{coll} = 5.5 kcal mol^{-1}. Note that in the previous QCT/SRP-AM1 theoretical results[14] only reactive trajectories with HCl(j<6) were considered. Experimental values are from refs 3 and 5.

fraction of energy is deposited as translation. As noted in the Introduction, the fraction of energy deposited as internal energy of the ethyl radical, $\langle f_{int}(C_2H_5)\rangle$, presents experimental controversies. At a collision energy of 5.5 kcal mol^{-1}, recent experiments[6,9] reported significant $\langle f_{int}(C_2H_5)\rangle$, 22−35%, which contrasts with the small value, 7%, reported previously by Kandel et al.[3,4] Our QCT/PES-2017 results show a value of 27%, in accordance with the most recent experiments. At a collision energy of 6.7 kcal mol^{-1}, the QCT/PES-2017 and experimental[9] results show a practically quantitative agreement. In sum, the ethyl radical presents a significant internal energy (with 85% as rotation) and so it has a significant role in the dynamics of the reaction.

3C. Product Rotational Distribution (PRD). The HCl(v=0,j) rotational distribution is plotted in Figure 3 at a collision energy of 5.5 kcal mol^{-1} for comparison with experiments.[3,5] Kandel et al.[3] and Rudic et al.[5] found experimentally cold HCl(v=0,j) rotational distribution, peaking at j = 1. The QCT/PES-2017 results reproduced this behavior, although they are hotter by one unity and broader. Note, however, that the difference in energy for j = 1 and 2 is only of 0.12 kcal mol^{-1}. Cold rotation is associated with linear C···H′···Cl transition states, which generate little torque during the reaction, whereas the broad distribution is associated with known drawbacks of the QCT method,[29−34] which tends to give large tails in these distributions and, therefore, hotter and broader rotational excitations. Note that the QCT/PES-2017 results noticeably improve previous QCT results,[14] which showed hotter rotational distributions, peaking at j = 3−4.

3D. Product Translational Distribution (PTD). The QCT/PES-2017 results at collision energies of 5.5 and 6.7 kcal mol^{-1} are shown in Figure 4, together with the experimental data for comparison.[3,6,9] At 5.5 kcal mol^{-1} Kandel etal.[3] and Bass et al.[6] used the photoloc technique to analyze the experimental measures, reporting the laboratory (LAB) frame speed distribution of the HCl(v=0,j=1) state, peaking between 1200 and 1600 m s^{-1}. Our QCT/PES-2017 results [in this case HCl(v=0,j=2) because it is the most populated level, see Figure 3] give a hotter distribution, peaking between 1700 and 1800 m s^{-1}. The good agreement obtained by Fernandez-Ramos et al.[11] using QCT calculations on a semiempirical PES is possibly fortuitous, because the comparison with experiment was not performed on the same footing: thus, though experimentally only the HCl(v=0,j=1) state was measured, theoretically all rotational states were considered and the violation of the ZPE in the products was not taken into account. However, the QCT/SRP-AM1 results by Greaves et al.[14] are accord with the present ones, with a wider distribution. At 6.7 kcal mol^{-1}, however, the QCT/PES-2017 results reproduce practically quantitatively the experimental measures.[9] Given the finer experimental conditions used in this latter case and the inherent problems with the photoloc technique, we suggest that the first experiments at 5.5 kcal mol^{-1} should be revised, and we suspect that a higher LAB-frame speed distribution will be found.

3E. Product Angular Distribution (PAD). Experimentally, Zare et al.[3] and Bass et al.[6] measured the differential cross section (DCS) for the reactive HCl(v=0,j) product at E_{coll} = 5.5 kcal mol^{-1} and found that whereas at low j values (j = 1, 3) the scattering distribution is practically isotropic, at higher j values

Table 1. Product Energy Fraction (%) for the Cl + C_2H_6 Reaction at 5.5 and 6.7 kcal mol^{-1}, with HCl(v=0)

	E_{coll} = 5.5 kcal mol^{-1}					E_{coll} = 6.7 kcal mol^{-1}	
	PES-2017[a]	Kandel[b]	Bass[c]	Huang[d]	Rudic[e]	PES-2017[a]	Huang[d]
f_r(HCl)[f]	6	2	2	3	3	6	2
$f_{int}(C_2H_5)$	27	7	22	35	19	27	30
f_t	67	91	76	63	78	67	68

[a]QCT/PES-2017 in the present work. [b]References 3 and 4. [c]Reference 6. [d]Reference 9. [e]Reference 12. [f]f_r(HCl), $f_{int}(C_2H_5)$, and f_t are, respectively, the fraction of the available energy as rotation in the HCl(v = 0) product, as internal energy in the ethyl radical coproduct, and as relative translation. This internal energy in the ethyl radical is distributed in rotation and vibration: 23% and 4%, respectively, at both collision energies.

DOI: 10.1021/acs.jpca.8b00149
J. Phys. Chem. A 2018, 122, 2626−2633

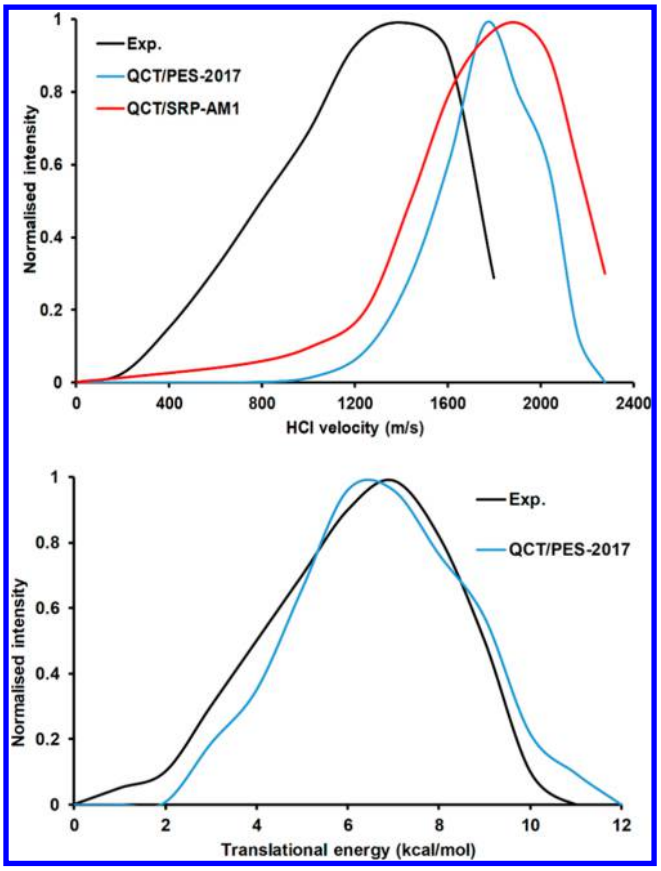

Figure 4. Upper panel: LAB-frame velocity distribution of HCl(v=0,j) in m s^{-1} at E_{coll} = 5.5 kcal mol^{-1}. Black line, experimental values from refs 3 and 6 using j = 1. Red line, theoretical QCT/SRP-AM1 results from ref 14 using j = 0−6. Blue line, present QCT/PES-2017 results using j = 2. The three series are normalized to unity. Lower panel: product translational distribution (kcal mol^{-1}) at a collision energy of 6.7 kcal mol^{-1}. Black and blue lines correspond, respectively, to the experimental data from ref 9 and to the present QCT/PES-2017 results. Both series are normalized to unity and correspond to the HCl(v=0,j=0−5) states.

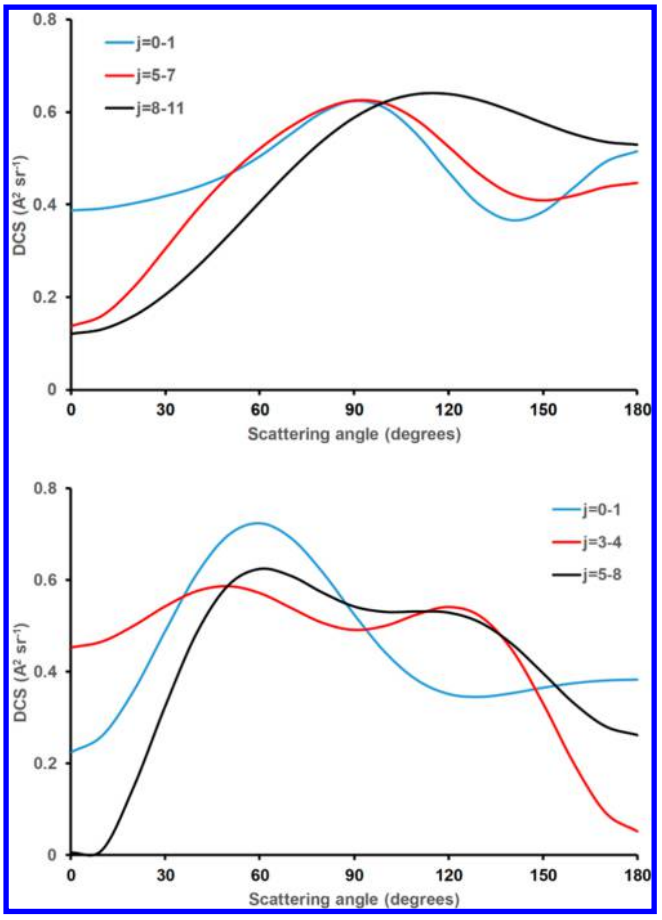

Figure 5. HCl(v=0,j) product angular distribution (with respect to the incident Cl atom) for the Cl + C_2H_6 reaction, normalized to unity by the factor ($2\pi/\sigma_r$). Upper and lower panels show the QCT/PES-2017 results at 5.5 and 6.7 kcal mol^{-1}, respectively.

(j = 6, 8) this distribution shifts toward backscattering. Figure 5 (upper panel) shows the QCT/PES-2017 DCS for the HCl(v=0,j) product with respect to the chlorine reactant. Note that due to the reduction of reactive trajectories for each individual j value, for this comparison with experiment we consider the HCl(v=0,j=0−1,j=5−7,j=8−11) states as examples of low, medium, and high j values, respectively. These calculations reproduce the experimental behavior, evolving from isotropic to backward scattering distribution with the increases of j.

At 6.7 kcal mol^{-1}, Suits and co-workers[8,9] measured the PAD for the HCl(v=0,j) product by studying also the effect of the rotational states and found similar results: the scattering distribution shifts from isotropic-sideway to backward with the value of j. Again we reproduce this behavior (Figure 5, lower panel) with the QCT/PES-2017 results, where the rotational states HCl(v=0,j=0−1,3−4,5−8) were considered to avoid statistical problems.

Taking into account all the rotational states, the scattering distributions are practically isotropic with a slightly sideways tendency for both collision energies. To analyze the influence of the impact parameter, b, Figure 6 shows the opacity functions (reaction probability versus b) for both collision

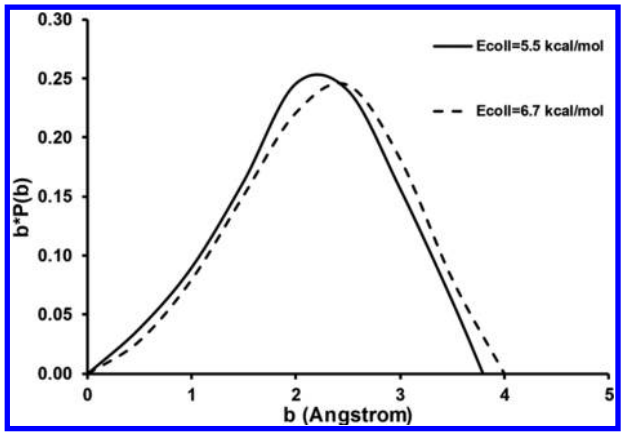

Figure 6. Opacity functions (reaction probability versus impact parameter) for the title reaction at collision energies of 5.5 and 6.7 kcal mol^{-1}.

energies, 5.5 and 6.7 kcal mol^{-1}. In both cases, the contribution from different b values is small (maximum of 25%), with the larger contributions from intermediate impact parameters, favoring sideways scattering.

Finally, to explain the high ethyl internal energy, we analyzed different correlations among the dynamics properties previously studied. Thus, we found coupling of ethyl internal energy (section 3B) with PTD (section 3D), which is shown in Figure

DOI: 10.1021/acs.jpca.8b00149
J. Phys. Chem. A 2018, 122, 2626−2633

7, and with PAD (section 3E), which is shown in Figure 8. We begin analyzing Figure 7, where an inverse lineal relation

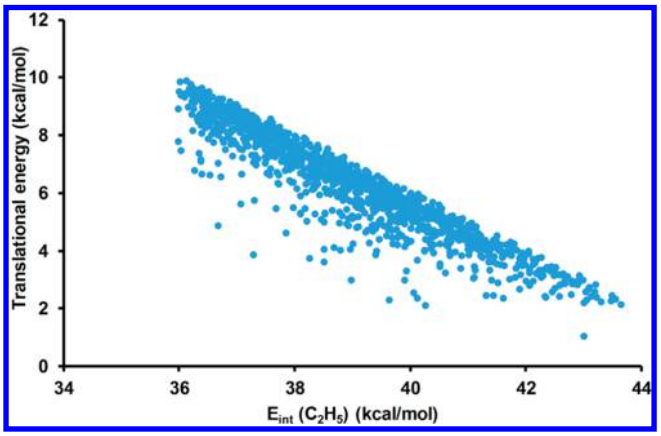

Figure 7. Correlation between the internal energy of the ethyl radical and the translational energy. Values in kcal mol^{-1}.

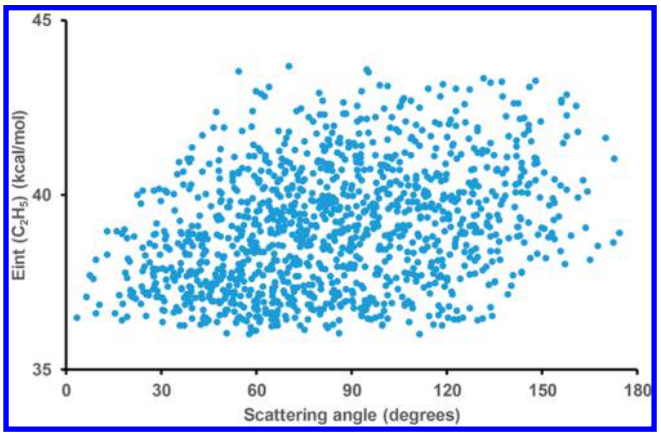

Figure 8. Correlation between the internal energy of the ethyl radical (kcal mol^{-1}) and the scattering angle (degrees).

between translational energy and ethyl radical internal energy is observed, i.e., a clear translational to internal energy transfer. With respect to the second coupling (Figure 8), a wide dispersion of values exists, although the tendency is clear. The forward scattered products are associated with large impact parameters via a stripping mechanism and the C_2H_5 product presents low internal energy. Conversely, high values of the ethyl internal energy are associated with small impact parameters, which lead to a rebound mechanism and backward scattered products. In this case, it seems that a more effective momentum change along the reactive process occurs, providing additional torque on the ethyl skeleton, increasing its internal energy. This effect has been previously reported in similar reactions, Cl + propane[35] and Cl + *n*-pentane.[36]

3F. "Chattering" Mechanism. Suits and co-workers[8,9] reported a bimodal PTD at the backward scattering region. They suggested that the faster component, $E_{trans} \sim 8-10$ kcal mol^{-1}, was associated with a direct reaction mechanism and low ethyl radical internal energy, and the slower component, $E_{trans} \sim 3-5$ kcal mol^{-1}, with high ethyl internal energy, was associated with an indirect "chattering" mechanism, where the H atom is temporarily trapped and rattles forth and back between the C and Cl atoms in the transition state. These authors noted that the overall contribution of "chattering" is small, less than 10%, in the collision energy range 3−10 kcal mol^{-1}, decreasing with collision energy. They suggested that the high internal energy excitation of the ethyl product is due to the fact that the reactive trajectories deviate significantly from the MEP, which has been also observed previously in the formaldehyde photodissociation[37] and the H + HBr reaction.[38] Later, Greaves et al.[13,14] performed QCT calculations at a collision energy of 5.5 kcal mol^{-1} to examine the validity of this mechanism at the backward scattering region. They observed that only about 3% of reactive trajectories (16% if only the reactive trajectories in the backward hemisphere are analyzed) presented oscillations of the H atom between C and Cl, but contrary to Suits and co-workers's results, the bimodal PTD was not found, and so direct and indirect "chattering" mechanisms showed similar PTDs.

However, before continuing, it is necessary at this point to analyze the role of the intermediate complexes in reactivity. It is well-known that trapped trajectories are usually associated with deep reactant and/or product wells, which is not the case for the present reaction, especially in the reactant channel with a shallow well, −1.14 kcal mol^{-1}. Thus, in fact, we reported indirect mechanisms in the study of the $Cl(^2P) + NH_3$ reaction.[39−41] This hydrogen abstraction reaction presents a barrier height $\Delta H(0K) = +1.7$ kcal mol^{-1}, with deep reactant, $\Delta H(0K) = -6.4$ kcal mol^{-1}, and product, $\Delta H(0K) = -5.1$ kcal mol^{-1}, wells, and the contribution of the indirect mechanism varies from 90% to 15% at collision energies of 1.0 and 3.0 kcal mol^{-1}, respectively. In this indirect mechanism the Cl and NH_3 reactants undergo repeated collisions in the wells and after a certain time the products separate. During these collisions translational, rotational, and vibrational energy transfer occurs. Clearly, these deep wells are not present in the title reaction.

To study this suggested mechanism, we performed additional batches of 10^5 trajectories where the maximum impact parameter was fixed at $b_{max} = 0.75$ Å to enhance the trajectories in the backward region and to better simulate the experimental conditions. This choice was motived by the inverse relation between impact parameter and scattering angle (Figure 9). The choice of the collision energy, however, merits a comment. Figure 10 shows schematic energy diagrams of the minimum energy path, MEP, and the vibrationally adiabatic path, V_a^G, i.e.,

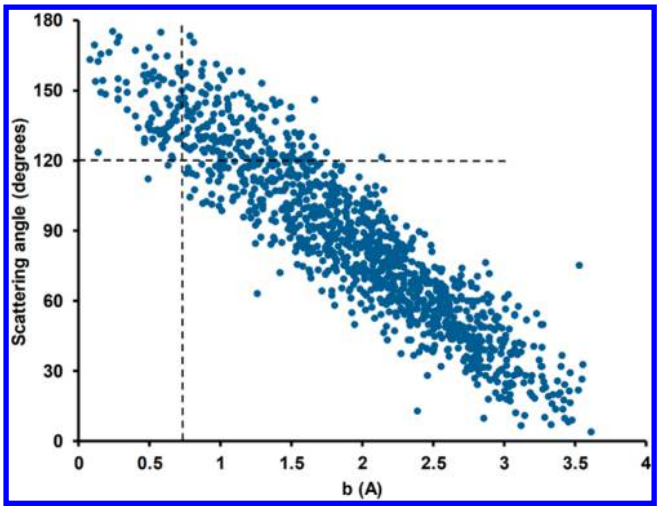

Figure 9. Correlation between the impact parameter, *b* in Å, and the scattering angle of the HCl product with respect to the incoming Cl atom.

DOI: 10.1021/acs.jpca.8b00149
J. Phys. Chem. A 2018, 122, 2626−2633

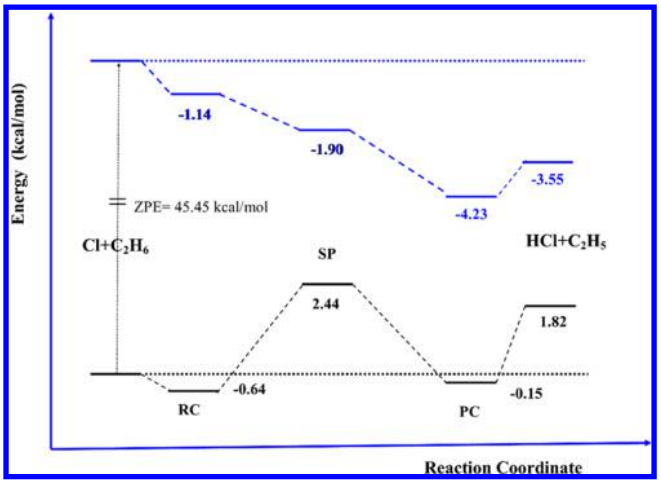

Figure 10. Schematic energy diagram of the minimum energy path (black line) and vibrationally adiabatic path (blue line), which includes the ZPE. Values in kcal mol^{-1} with respect to their respective energy in the reactants (level zero, dotted lines).

when the ZPE is included, V_a^G = MEP + ZPE. In this latter case, all stationary points are below the Cl + C_2H_6 reactants, so the barrier is "submerged", $\Delta H(0K) = -1.90$ kcal mol^{-1}. In these energetic conditions we believe that high collision energies do not favor trapping in the shallow and "submerged" wells. In fact, at E_{coll} = 6.7 kcal mol^{-1}, where Suits and co-workers reported 7.6% of contribution of the "chattering" mechanism, we found that all trajectories were direct. Thus, we tried with a lower collision energy, 2.0 kcal mol^{-1} (10^5 trajectories with b_{max} = 0.75 Å). Again, our QCT/PES-2017 results led to direct mechanisms, where a brief encounter between the reactants was observed, forming the HCl product which immediately recoiled away. In sum, as was previously noted, we observe an inverse relation between the translational energy and the ethyl radical internal energy (Figure 7), at both collision energies, 6.7 and 2.0 kcal mol^{-1}, i.e., a clear translational to internal energy transfer, although without bimodal PTDs.

4. CONCLUSIONS

To understand the dynamics behavior of the polyatomic Cl + C_2H_6 hydrogen abstraction reaction and to reproduce the available experimental information, which presents in some cases controversies between different laboratories, in the present work we perform QCT calculations on a recently developed full-dimensional surface, PES-2017. To make a rigorous theoretical/experimental comparison, we included pseudoquantization in the reactant and product analysis, discarding those reactive trajectories whose results did not meet quantum mechanical requirements, the ZPE violation problem, and additional stringent constraints in the QCT outcome to analyze exclusively the product experimentally detected, HCl(v=0,j) vibrational ground state.

For years a controversy on the role of the ethyl radical in dynamics has existed. Though the first experimental studies concluded that it acts as a pseudoatom, as a spectator, subsequent studies (both theoretical and experimental) have reported significant internal energy, mainly as rotation, emphasizing its active role. The present QCT/PES-2017 results support this last finding, with significant internal energy, 27%.

The largest fraction of available energy is deposited as translation, 67%, with cold rotational distribution of the HCl(v=0,j) product. These results reproduce the experimental evidence and are consistent with the kinematic and topology of the reactive system, characterized by a heavy-light-heavy mass combination and a linear and tight transition state.

Experimental studies of the HCl(v=0,j) scattering distribution report a clear shift from isotropic to backward hemisphere with the increases in the j number. The present QCT/PES-2017 results reproduce this tendency in this sensitive dynamics property, thus giving confidence to the quality of the new PES.

With respect to product translational distribution we found different agreement with the experimental measures at 5.5 kcal mol^{-1} (by using the photoloc technique and considering the ethyl radical as a spectator) and the most recent at 6.7 kcal mol^{-1}. Although at 6.7 kcal mol^{-1} the theoretical/experimental agreement is practically quantitative, at 5.5 kcal mol^{-1} our distribution is slightly hotter. Given the good agreement at the higher collision energy and that at the lower energy the internal energy of the ethyl radical is despised, we suggest that this last result should be revised. In addition, Suits and co-workers at 6.7 kcal mol^{-1} experimentally reported a bimodal PTD in the backward scattering hemisphere of the HCl(v=0,j=2) state, suggesting an indirect "chattering" mechanism to explain the internal energy of the ethyl radical, where the ethyl internal energy is associated with reactive trajectories which deviate from the minimum energy path. Our QCT/PES-2017 results did not find any evidence of this mechanism, although a clear translational to internal energy transfer was observed.

Finally, from the number of trajectories run, the collision energies analyzed, and the more rigorous analysis of the QCT results, which gives a theoretical/experimental comparison on the same footing, the present results noticeably improve previous theoretical studies on the title reaction.

AUTHOR INFORMATION

Corresponding Author

*J. Espinosa-Garcia. E-mail: joaquin@unex.es.

ORCID

Joaquin Espinosa-Garcia: 0000-0002-0058-8727

Emilio Martinez-Nuñez: 0000-0001-6221-4977

Notes

The authors declare no competing financial interest.

ACKNOWLEDGMENTS

This work was partially supported by Gobierno de Extremadura, Spain (Project No. GR15015). We thank Jose C. Corchado for computational support.

REFERENCES

(1) Rangel, C.; Espinosa-Garcia, J. Full-dimensional Analytical Potential Energy Surface Describing the Gas-phase Cl + C_2H_6 Reaction and Kinetics Study of Rate Constants and Kinetic Isotope Effects. *Phys. Chem. Chem. Phys.* **2018**, *20*, 3925.

(2) Polanyi, J. C. Concepts in Reaction Dynamics. *Acc. Chem. Res.* **1972**, *5*, 161−168.

(3) Kandel, S. A.; Rakitzis, T. P.; Lev-On, T.; Zare, R. N. Dynamics for the Cl+C_2H_6 →HCl+C_2H_5 Reaction Examined Through State-Specific Angular Distributions. *J. Chem. Phys.* **1996**, *105*, 7550−7559.

(4) Kandel, S. A.; Rakitzis, T. P.; Lev-On, T.; Zare, R. N. Angular Distributions for the Cl+C_2H_6 →HCl+C_2H_5 Reaction Observed via Multiphoton Ionization of the C_2H_5 Radical. *J. Phys. Chem. A* **1998**, *102*, 2270−2273.

DOI: 10.1021/acs.jpca.8b00149
J. Phys. Chem. A 2018, 122, 2626−2633

(5) Rudic, S.; Ascenzi, D.; Orr-Ewing, A. J. Rotational Distribution of the HCl Products from the Reaction of Cl(^{2}P) Atoms with Methanol. *Chem. Phys. Lett.* **2000**, *332*, 487−495.
(6) Bass, M. J.; Brouard, M.; Willante, C.; Kitsppoulos, T. N.; Samartzis, P. C.; Toomes, R. L. The Dynamics of the Cl+C_2H_6 →HCl +C_2H_5 Reaction at 0.24 eV: Is Ethyl a Spectator? *J. Chem. Phys.* **2003**, *119*, 7168−7178.
(7) Toomes, R. L.; Kitsopoulos, T. N. Rotationally Resolved Reaction Product Imaging using Crossed Molecular Beams. *Phys. Chem. Chem. Phys.* **2003**, *5*, 2481−2483.
(8) Li, W.; Huang, C.; Patel, M.; Wilson, D.; Suits, A. G. State-resolved Reactive Scattering by Slice Imaging: A New View of the Cl +C_2H_6 Reaction. *J. Chem. Phys.* **2006**, *124*, 011102.
(9) Huang, C.; Li, W.; Suits, A. G. Rotationally Resolved Reactive Scattering: Imaging Detailed Cl+C_2H_6 Reaction Dynamics. *J. Chem. Phys.* **2006**, *125*, 133107.
(10) Pearce, J. K.; Retail, B.; Greaves, S. J.; Rose, R. A.; Orr-Ewing, A. J. Imaging the Dynamics of Reactions between Cl Atoms and the Cyclic Ethers Oxirane and Oxetane. *J. Phys. Chem. A* **2007**, *111*, 13296−13304.
(11) Fernandez-Ramos, A.; Martinez-Nuñez, E.; Marques, J. M. S.; Vazquez, S. A. Dynamics Calculations for the Abstraction Reaction: Thermal Rate Constants and Kinetic Isotope Effects. *J. Chem. Phys.* **2003**, *118*, 6280−6288.
(12) Rudic, S.; Murray, C.; Harvey, J. N.; Orr-Ewing, A. J. On-the-fly Ab Initio Trajectory Calculations of the Dynamics of Cl Atom Reactions with Methane, Ethane and Methanol. *J. Chem. Phys.* **2004**, *120*, 186−198.
(13) Greaves, S. J.; Kim, J.; Orr-Ewing, A. J.; et al. Studying 'Chattering Collisions' in the Cl + Ethane Reaction with Classical Trajectories. *Chem. Phys. Lett.* **2007**, *441*, 171−175.
(14) Greaves, J.; Orr-Ewing, A. J.; Troya, D. Classical Trajectory Study of the Dynamics of the Reaction of Cl Atoms with Ethane. *J. Phys. Chem. A* **2008**, *112*, 9387−9395.
(15) Chase, M. W., Jr.; Davies, C. A.; Downey, J. R.; Frurip, D. J.; McDonald, R. A.; Syverud, A. N. *JANAF Thermochemical Tables*, 3rd ed.; National Bureau of Standards, Washington, D.C., 1985; Vol. *14*.
(16) Atkinson, R.; Baulch, D. L.; Cox, R. A.; Crowley, J. N.; Hampson, R. F., Jr.; Kerr, J. A.; Rossi, M. J.; Troe, J. *Summary of Evaluated Kinetic and Photochemical Data for Atmospheric Chemistry*; IUPAC, 2003, Web version: http://www.iupac-kinetic.ch.cam.ac.uk.
(17) Hu, X.; Hase, W. L.; Pirraglia, Y. Vectorization of the General Monte Carlo Classical Trajectory Program VENUS. *J. Comput. Chem.* **1991**, *12*, 1014−1024.
(18) Hase, W. L.; Duchovic, R. J.; Hu, X.; Komornicki, A.; Lim, K. F.; Lu, D-h.; Peslherbe, G. H.; Swamy, K. N.; Van de Linde, S. R.; Varandas, A. J. C.; et al. VENUS96: A General Chemical Dynamics Computer Program. *QCPE Bull.* **1996**, *16*, 43.
(19) Zhang, B.; Shiu, W.; Lin, J. J.; Liu, K. Mode Correlation of Product Pair in the Reaction OH + CD_4 → HOD + CD_3. *J. Chem. Phys.* **2005**, *122*, 131102.
(20) Zhang, B.; Shiu, W.; Lin, J. J.; Liu, K. Imaging the Reaction Dynamics of OH + CD_4. 2. Translational Energy Dependencies. *J. Phys. Chem. A* **2005**, *109*, 8983−8988.
(21) Zhang, B.; Shiu, W.; Lin, J. J.; Liu, K. Imaging the Reaction Dynamics of OH + CD_4. 3. Isotopic Effects. *J. Phys. Chem. A* **2005**, *109*, 8989−8993.
(22) Zhang, W.; Kawamata, H.; Liu, K. C-H Stretching Excitation in the Early Barrier F + CHD_3 Reaction Inhibits C-H Bond Cleavage. *Science* **2009**, *325*, 303−306.
(23) Yang, J.; Zhang, D.; Jiang, B.; Dai, D.; Wu, G.; Zhang, D.; Yang, X. How Is CH Vibrational Energy Redistributed in F + $CHD_3(\nu_1 = 1)$ → HF + CD_3 ? *J. Phys. Chem. Lett.* **2014**, *5*, 1790−1794.
(24) Yang, J.; Zhang, D.; Chen, Z.; Blauert, F.; Jiang, B.; Dai, D.; Wu, G.; Zhang, D.; Yang, X. Effect of the CH Stretching Excitation on the Reaction Dynamics of F + CHD_3 → DF + CHD_2. *J. Chem. Phys.* **2015**, *143*, 044316.
(25) Bonnet, L.; Corchado, J. C.; Espinosa-Garcia, J. Pair-correlated Speed Distributions for the OH+CH_4/CD_4 Reactions: Further Remarks on their Classical Trajectory Calculations in a Quantum Spirit. *C. R. Chim.* **2016**, *19*, 571−578.
(26) Bonnet, L.; Espinosa-Garcia, J. Simulation of the Experimental Imaging Results for the OH + CHD_3 Reaction with a Simple and Accurate Theoretical Approach. *Phys. Chem. Chem. Phys.* **2017**, *19*, 20267−20270.
(27) Espinosa-Garcia, J.; Bonnet, L.; Corchado, J. C. Theoretical Study of the Pair-Correlated F + $CHD_3(v = 0, \nu_1 = 1)$ Reaction: Effect of CH Stretching Vibrational Excitation. *J. Phys. Chem. A* **2017**, *121*, 4076−4092.
(28) Truhlar, D. G.; Blais, N. C. Legendre Moment Method for Calculating Differential Scattering Cross Sections from Classical Trajectories with Monte Carlo Initial Conditions. *J. Chem. Phys.* **1977**, *67*, 1532−1539.
(29) Gerrity, D. P.; Valentini, J. J. Experimental Study of the Dynamics of the H+D_2→HD+D Reaction at Collision Energies of 0.55 and 1.30 eV. *J. Chem. Phys.* **1984**, *81*, 1298−1313.
(30) Kliner, D. A. V.; Rinnen, K. D.; Zare, R. N. The D+H_2 Reaction: Comparison of Experiment with Quantum-mechanical and Quasi-classical Calculations. *Chem. Phys. Lett.* **1990**, *166*, 107−111.
(31) Bean, B. D.; Fernández-Alonso, F.; Zare, R. N. Distribution of Rovibrational Product States for the "Prompt" Reaction H + D_2(v = 0, j = 0−4) → HD(v′ = 1,2,j′) + D near 1.6 eV Collision Energy. *J. Phys. Chem. A* **2001**, *105*, 2228−2233.
(32) Bean, B. D.; Ayers, J. D.; Fernandez-Alonso, F.; Zare, R. N. State-resolved Differential and Integral Cross Sections for the Reaction H+D_2→HD(v′=3,j′=0−7)+D at 1.64 eV Collision Energy. *J. Chem. Phys.* **2002**, *116*, 6634−6639.
(33) Pomerantz, A. E.; Ausfelder, F.; Zare, R. N.; Althorpe, S. C.; Aoiz, F. J.; Bañares, L.; Castillo, J. F. Disagreement Between Theory and Experiment in the Simplest Chemical Reaction: Collision Energy Dependent Rotational Distributions for H+D_2→HD(ν'=3,j′) + D. *J. Chem. Phys.* **2004**, *120*, 3244−3254.
(34) Xie, T.; Bowman, J. M.; Duff, J. W.; Braunstein, M.; Ramachandran, B. Quantum and Quasiclassical Studies of the O(^{3}P) + HCl→OH + Cl(^{2}P) Reaction Using Benchmark Potential Surfaces. *J. Chem. Phys.* **2005**, *122*, 014301.
(35) Blank, D. A.; Hemmi, N.; Suits, A. G.; Lee, Y. T. A Crossed Molecular Beam Investigation of the Reaction Cl + Propane →HCl + C_3H_7 using VUV Synchrotron Radiation as a Product Probe. *Chem. Phys.* **1998**, *231*, 261−278.
(36) Hemmi, N.; Suits, A. G. The Dynamics of Hydrogen Abstraction Reactions: Crossed-Beam Reaction Cl + n-C_5H_{12} → C_5H_{11} + HCl. *J. Chem. Phys.* **1998**, *109*, 5338−5343.
(37) Townsend, D.; Lahankar, S. A.; Lee, S. K.; Chambreau, S. D.; Suits, A. G.; Zhang, X.; Rheinecker, J.; Harding, L. B.; Bowman, J. M. The Roaming Atom: Straying from the Reaction Path in Formaldehyde Decomposition. *Science* **2004**, *306*, 1158−1161.
(38) Pomerantz, A. E.; Camden, J. P.; Chiou, A. S.; Ausfelder, F.; Chawla, N.; Hase, W. L.; Zare, R. N. Reaction Products with Internal Energy beyond the Kinematic Limit Result from Trajectories Far from the Minimum Energy Path: An Example from H + HBr → H_2 + Br. *J. Am. Chem. Soc.* **2005**, *127*, 16368−16369.
(39) Monge-Palacios, M.; Rangel, C.; Corchado, J. C.; Espinosa-Garcia, J. Analytical Potential Energy Surface for the Reaction with Intermediate Complexes NH_3 + Cl → NH_2 + HCl: Application to the Kinetics Study. *Int. J. Quantum Chem.* **2012**, *112*, 1887−1903.
(40) Monge-Palacios, M.; Yang, M.; Espinosa-Garcia, J. QCT and QM Calculations of the Cl(^{2}P) + NH_3 Reaction: Influence of the Reactant Well on the Dynamics. *Phys. Chem. Chem. Phys.* **2012**, *14*, 4824−4834.
(41) Monge-Palacios, M.; Corchado, J. C.; Espinosa-Garcia, J. Quasi-classical Trajectory Study of the Role of Vibrational and Translational Energy in the Cl(^{2}P) + NH_3 Reaction. *Phys. Chem. Chem. Phys.* **2012**, *14*, 7497−7508.

DOI: 10.1021/acs.jpca.8b00149
J. Phys. Chem. A 2018, 122, 2626−2633